ROLE OF PORE-SCALE HETEROGENEITY ON REACTIVE FLOWS IN POROUS MATERIALS: VALIDITY OF THE CONTINUUM REPRESENTATION OF REACTIVE TRANSPORT

PETER C. LICHTNER[1], QINJUN KANG[1]

[1]Los Alamos National Laboratory, Earth and Environmental Sciences, Hydrology, Geochemistry and Geology Group, Los Alamos, NM 87545, USA (lichtner@lanl.gov, qkang@lanl.gov).

ABSTRACT

The Lattice Boltzmann (LB) model for multi-component reactive transport in porous media is used to investigate the role of spatial heterogeneity related to pore geometry on mass transport and reaction rates in porous materials and its impact on the validity of the continuum representation of reactive transport. Because of the ability of the LB model to accurately represent pore-scale phenomena, it affords the most comprehensive approach to investigate the influence of pore-scale heterogeneity on continuum formulations of reactive transport. We apply the LB model to various simple, hypothetical chemical systems in a set of two-dimensional, artificially-constructed fractured media. The reactive-transport processes are simulated at the pore scale, with systematic consideration of the pore-scale flow field, diffusion, homogeneous reactions among multiple aqueous species, heterogeneous reactions between the aqueous solution and minerals, as well as the resulting changes in solid and pore geometry. The results are averaged over vertical slabs taken as representative elemental volumes (REVs), and compared with one- and two-dimensional continuum-scale simulations.

1. INTRODUCTION

Continuum models are based on spatial averages taken over length scales much larger than typical particle sizes and as a result spatial heterogeneity at smaller scales is unresolved. This loss of information includes pore-scale velocities and geometry, mineral texture, and other features. Therefore, understanding the impact of pore-scale spatial heterogeneity on reactive processes in porous materials is a key aspect in validating continuum description of reactive transport and developing predictive capabilities of system behavior. The continuum- and pore-scale equations involve different physics. Pore-scale phenomena is governed by the Navier-Stokes and pore-scale advective-diffusion-reaction equations. These equations account for pore-scale velocity fluctuations, local concentration gradients, and reactions with solids at the pore fluid-solid interface. The upscaled form of the pore-scale conservation equations are the continuum-scale Darcy-based flow and transport equations. The continuum-scale transport equations incorporate advection averaged over many pore volumes, and molecular diffusion through an effective diffusion coefficient. An term representing dispersion caused by mixing of fluid at the pore scale must generally be added to the continuum transport equations. Solid reactions are incorporated through a volumetric averaged reaction rate taken over a control volume, referred to as a representative elemental volume (REV) which is assumed to characterize the continuum-scale properties of the system. By contrast, the pore-scale reactive transport equations incorporate heterogeneous reactions as boundary conditions at the fluid-solid interface.

As reactions proceed, the pore-scale equations account for changes in pore geometry which in turn may alter the flow field. The continuum equations are insensitive to the details of the pore geometry and mineral texture. The continuum-scale flow and transport equations involve various effective continuum parameters such as permeability, dispersivity, tortuosity, and specific mineral surface area. One of the goals of performing pore-scale simulations is to obtain values for these continuum parameters through upscaling the pore-scale results.

In this study we apply a Lattice Boltzmann (LB) model to investigate multi-component reactive transport at the pore scale [Kang et al., 2004, 2005, 2006]. By comparing the pore-scale results averaged over a REV to continuum scale models the validity of volume averaging can be ascertained for complex pore geometries. Through upscaling pore-scale processes to the continuum scale it is possible to identify key parameters and physicochemical processes that control macroscopic phenomena and simultaneously provide constitutive relations needed in continuum models. We hypothesize that pore-scale simulations will enable the most appropriate continuum model—single or dual continuum—to be determined, or will demonstrate that upscaling is in fact not possible, for example, as is expected in the presence of reaction instabilities resulting in wormhole formation. In cases where upscaling is shown to be valid, pore-scale simulations can provide appropriate values for macro-scale properties of the porous medium such as primary and secondary flow domains and interfacial area, permeability, tortuosity, dispersivity, and reactive surface area.

2. Multi-Scale Continuum Formulation of Reactive Transport

Multiscale processes range from millimeter scales or smaller to macroscales of tens of meters or larger. Capturing this extreme range of scales is impossible with current and near-future computing capabilities employing conventional single continuum models with simple orthogonal grids. For example, discretizing a computational domain measuring 2 km $\times$ 1 km $\times$ 500 m = 10^9 m^3, into cubic millimeter nodes would require 10^{18} computational nodes to describe. Reducing the grid spacing by just a factor of 10 in each dimension of a 3D domain, increases the number of nodes by a factor of 1000. One promising approach is to incorporate a sub-grid scale model that can account for millimeter scales into the primary-grid continuum model. This approach is commonly used to describe fractured porous media based on a dual continuum representation as a special case of a sub-grid model, but the concept applies more generally to multiscale media represented by multiple interacting continua. This work is focused on upscaling a pore-scale LB model to the continuum scale by implementing a sub-grid scale model at the continuum scale. In this preliminary study, idealized synthetic media are used.

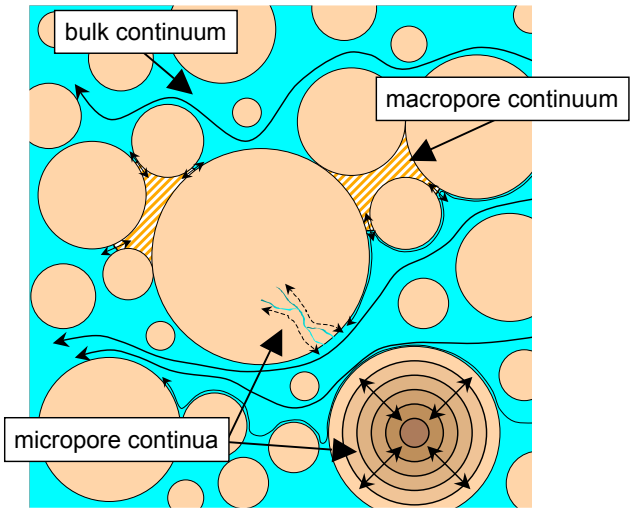

Figure 1. Schematic of pore scale geometry and transport pathways.

2.1. **Geometry.** To define a multi-scale porous medium, the control volume V is presumed to consist of bulk and matrix domains with volumes V_b and V_m, respectively, satisfying

$$V \;=\; V_b + V_m. \tag{1}$$

The fraction of the control volume occupied by the bulk domain and its intrinsic porosity are equal to

$$\epsilon_b \;=\; \frac{V_b}{V}, \qquad \varphi_b \;=\; \frac{V_b^p}{V_b}, \tag{2}$$

respectively.

If the matrix volume is composed of particles with volume V_m^0 and associated area A_m^0, the number of particles within a control volume is given by

$$N \;=\; \frac{V_m}{V_m^0} \;=\; \frac{1-\epsilon_b}{V_m^0}V, \tag{3}$$

and the interfacial area between bulk and matrix domains per unit volume is equal to

$$A_{mb} \;=\; \frac{N}{V}A_m^0 \;=\; (1-\epsilon_b)\frac{A_m^0}{V_m^0}. \tag{4}$$

For spheres and cubes it follows that

$$A_{mb} \;=\; \frac{N}{V}4\pi r_m^2 \;=\; \frac{3}{r_m}(1-\epsilon_b) \quad \text{(spheres)}, \tag{5}$$

$$\;=\; \frac{N}{V}6l_m^2 \;=\; \frac{6}{l_m}(1-\epsilon_b) \quad \text{(cubes)}. \tag{6}$$

Both bulk and matrix domains may contain solid and aqueous phases, with intrinsic porosities φ_b and φ_m, respectively.

In the general case, a control volume consists of several different particle types with different sizes, compositions, and physical properties such as porosity and tortuosity. The particle distribution is characterized by the parameters: $\{x_k,\, M_k^0,\, V_k^0,\, A_k^0\}$, giving the number fraction of particles of type k, its mass, volume and associated surface area. The number fraction x_k is defined by

$$x_k \;=\; \frac{N_k}{N}, \qquad N \;=\; \sum_k N_k, \tag{7}$$

where it is assumed that there are N_k particles of type k, with total number of particles N. Each particle type is characterized by its volume V_k^0, mass M_k^0, density $\rho_k^0 = M_k^0/V_k^0$, and surface area A_k^0, as well as transport properties including porosity φ_k and effective diffusivity D_k. In addition, different mineralogic compositions are also possible. The particle number density is given by the expression

$$\mathcal{N} \;=\; \frac{N}{V} \;=\; \frac{1-\epsilon_b}{\sum_k x_k V_k^0}. \tag{8}$$

The specific surface area of the kth particle type is given by

$$A_k \;=\; \mathcal{N}_k A_k^0 \;=\; \mathcal{N} x_k A_k^0 \;=\; \big(1-\epsilon_b\big)\frac{x_k A_k^0}{\sum_{k'} x_{k'} V_{k'}^0}. \tag{9}$$

2.2. **Multi-Scale Multicomponent Reactive Transport Equations.** Multi-scale, multicomponent continuum-scale mass reactive transport equations for primary species can be written in the general form as the set of coupled partial differential equations [Lichtner, 2000]

$$\frac{\partial}{\partial t}\epsilon_b\varphi_b\Psi_j^b + \boldsymbol{\nabla}\cdot\epsilon_b\boldsymbol{\Omega}_j^b \;=\; \sum_k \mathcal{N}_k A_{kb}\Omega_j^{kb} - \sum_s \nu_{js}A_s^b I_s^b, \tag{10}$$

for the bulk fluid, and

$$\frac{\partial}{\partial t}\varphi_k\Psi_j^k + \boldsymbol{\nabla}\cdot\boldsymbol{\Omega}_j^k \;=\; -\sum_s \nu_{js}A_s^k I_s^k, \tag{11}$$

for the matrix fluid associated with the kth particle, with volume averaged kinetic mineral reaction rates $I_s^{b,k} = -\kappa_s^{b,k}(1 - K_s Q_s^{b,k})$ based on transition state theory, with rate constant $\kappa_s^{b,k}$ and specific surface $A_s^{b,k}$. The total concentration and flux are defined, respectively, by [Lichtner, 1985, 1996]

$$\Psi_j^{b,k} \;=\; C_j^{b,k} + \sum_i \nu_{ji}C_i^{b,k}, \quad \boldsymbol{\Omega}_j^{b,k} \;=\; -\varphi_{b,k}D_{b,k}\boldsymbol{\nabla}\Psi_j^{b,k} + \boldsymbol{q}_{b,k}\Psi_j^{b,k}, \tag{12}$$

with effective diffusivity $D_{b,k}$ and Darcy flow rate $\boldsymbol{q}_{b,k}$, and with secondary species concentrations

$$C_i^{b,k} \;=\; K_i\big(\gamma_i^{b,k}\big)^{-1}\prod_j\big(\gamma_j^{b,k}C_j^{b,k}\big)^{\nu_{ji}}. \tag{13}$$

The boundary condition and flux at the bulk-matrix fluid interface are given by

$$C_j^k(r = r_k,\, t;\boldsymbol{r}) \;=\; C_j^b(\boldsymbol{r},\, t), \quad \Omega_j^{kb} \;=\; -\varphi_k D_k\left(\frac{\Psi_j^k - \Psi_j^b}{d_{kb}}\right). \tag{14}$$

The matrix equation is quite general and applies to various geometries including spheres and linear domains. As an approximation cubes and irregular shaped particles may be used. Because of computational considerations, the matrix domain equations are reduced to an equivalent 1D problem.

3. Pore-Scale Multicomponent Lattice Boltzmann Formulation

3.1. **Pore-Scale Mass Conservation Equations.** The LB method describes reactive flows in porous media equivalent to the Navier-Stokes and pore-scale advection-diffusion-reaction equations. For a multicomponent system these equations have the form

$$\frac{\partial\rho}{\partial t} + \boldsymbol{\nabla}\cdot(\rho\boldsymbol{u}) = 0, \quad \frac{\partial}{\partial t}(\rho\boldsymbol{u}) + \boldsymbol{\nabla}\cdot(\rho\boldsymbol{u}\boldsymbol{u}) = -\boldsymbol{\nabla}p + \boldsymbol{\nabla}\cdot\big[\rho\nu\big(\boldsymbol{\nabla}\boldsymbol{u} + \boldsymbol{u}\boldsymbol{\nabla}\big)\big], \tag{15}$$

and

$$\frac{\partial\Psi_j}{\partial t} + \boldsymbol{\nabla}\cdot\big(\boldsymbol{u}\Psi_j - D\boldsymbol{\nabla}\Psi_j\big) = 0, \quad D\frac{\partial\Psi_j}{\partial n} = \sum_s \nu_{js}I_s, \tag{16}$$

where p denotes the pressure, ρ the density, $\boldsymbol{u}$ velocity field, and ν the viscosity of the fluid, n the unit normal perpendicular to the fluid-mineral interface pointing towards the fluid phase, and Ψ_j denotes the total concentration of the jth primary species. These equations are subject to no flow boundary conditions at the pore walls that may be very complex due to the random geometry at the pore scale. In addition, the transport equation is subject boundaries conditions representing reactions with minerals at the pore-mineral interface.

The LB approach overcomes the difficulties of imposing no flow conditions by by using bounce-back boundary conditions at the pore walls for the particle-velocity-distribution function [Chen and Doolan, 1998]. The LB equations for flow and transport have the forms

$$f_\alpha(\boldsymbol{x} + \boldsymbol{e}_\alpha \delta t,\, t + \delta t) \;=\; f_\alpha(\boldsymbol{x},\, t) - \frac{f_\alpha(\boldsymbol{x},\, t) - f_\alpha^{\mathrm{eq}}(\rho,\, \boldsymbol{u})}{\tau_\nu}, \tag{17}$$

and

$$g_{\alpha j}(\boldsymbol{x} + \boldsymbol{e}_\alpha \delta t,\, t + \delta t) \;=\; g_{\alpha j}(\boldsymbol{x},\, t) - \frac{g_{\alpha j}(\boldsymbol{x},\, t) - g_{\alpha j}^{\mathrm{eq}}(\Psi_j,\, \boldsymbol{u})}{\tau_D}, \tag{18}$$

where the equilibrium distributions for flow and transport, $f_\alpha^{\mathrm{eq}}(\rho,\, \boldsymbol{u})$ and $g_{\alpha j}^{\mathrm{eq}}(\Psi_j,\, \boldsymbol{u})$, are defined by

$$f_\alpha^{\mathrm{eq}}(\rho,\, \boldsymbol{u}) = \omega_\alpha \rho F(\boldsymbol{u}),\; g_{\alpha j}^{\mathrm{eq}}(\Psi_j,\, \boldsymbol{u}) = \omega_\alpha \Psi_j F(\boldsymbol{u}),\; F(\boldsymbol{u}) = 1 + \frac{\boldsymbol{e}_\alpha \cdot \boldsymbol{u}}{RT} + \frac{(\boldsymbol{e}_\alpha \cdot \boldsymbol{u})^2}{2(RT)^2} - \frac{\boldsymbol{u} \cdot \boldsymbol{u}}{2RT}. \tag{19}$$

The velocities $\boldsymbol{e}_\alpha$ for the two dimensional, 9-speed, LB model are defined by

$$\boldsymbol{e}_\alpha \;=\; \begin{cases} 0, & \alpha = 0 \\ \big(\cos\big[\dfrac{(\alpha-1)\pi}{2}\big],\, \sin\big[\dfrac{(\alpha-1)\pi}{2}\big]\big), & \alpha = 1-4 \\ \sqrt{2}\big(\cos\big[\dfrac{(\alpha-5)\pi}{2} + \dfrac{\pi}{4}\big],\, \sin\big[\dfrac{(\alpha-5)\pi}{2} + \dfrac{\pi}{4}\big]\big), & \alpha = 5-8 \end{cases}, \tag{20}$$

with weight factors ω_α defined by $\omega_0 = 4/9; \omega_\alpha = 1/9, (\alpha = 1, 4); \omega_\alpha = 1/36, (\alpha = 5, 8)$. The fluid velocity and density, and solute concentration are related to the probability density functions by the equations

$$\rho = \sum_\alpha f_\alpha, \quad \boldsymbol{u} = \frac{1}{\rho} \sum_\alpha \boldsymbol{e}_\alpha f_\alpha, \quad \Psi_j = \sum_\alpha g_{\alpha j}. \tag{21}$$

For a given pore geometry, the LB method provides an accurate representation of the pore-scale velocity field. This is achieved through a relatively fine discretization of the pore space. However, more difficult is to obtain an accurate representation of the solid morphology because it can involve length scales much smaller than the pore scale, from sub-micron to nanometer scales. As a consequence of this, it is necessary to approximate the pore geometry at the smallest resolution possible within the framework of the LB model. One should note, however, that as length scales become smaller, diffusion times also become shorter, proportional to the square of the distance: $t \sim l^2/D$.

4. Applications

4.1. **Upscaling Pore Scale LBM Simulations.** The simplest upscaling approach is to volume average the LB result for the solute concentration over a REV and compare the resulting one-dimensional profile with single and dual continuum model results. The spatially averaged pore-scale concentration $\overline{\Psi}_j$ is defined as

$$\overline{\Psi}_j(\overline{x},\, t) \;=\; \frac{1}{V_{\mathrm{REV}}} \int_{V_{\mathrm{REV}}} \Psi_j(x',\, y',\, t)\, dx'\, dy', \tag{22}$$

where $\Psi_j(x,\, y,\, t)$ is the solution to the 2D LB equations for the solute concentration. The integral is taken over a REV for the bulk fluid system centered at $\overline{x}$, and excludes the matrix domain.

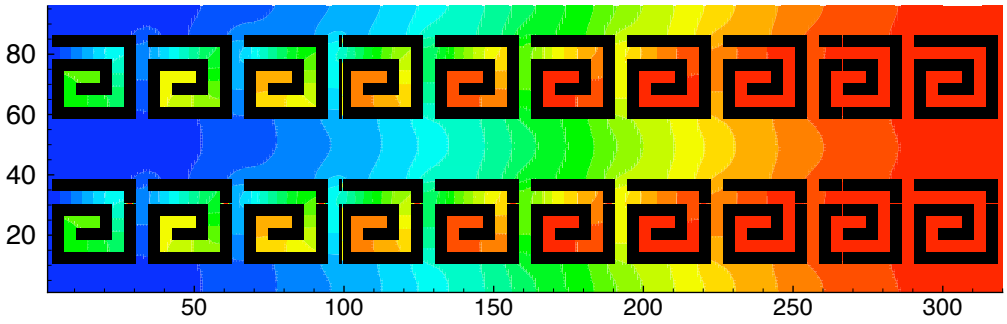

FIGURE 2. LB result for flow of a tracer through a porous medium with primary and secondary porosity.

To obtain the breakthrough concentration from the LB simulations, and flux-averaged concentration is used obtained from the experssion

$$<\Psi_j(t)> = \frac{\int \rho(L,\, y,\, t) v_x(L,\, y,\, t) \Psi_j(L,\, y,\, t)\, dy}{\int \rho(L,\, y',\, t) v_x(L,\, y',\, t)\, dy'}. \tag{23}$$

where L is the length of the column.

The LB model is applied to the two-dimensional system with the geometry shown in Figure 2. The system measures 320×96 lattice units. One lattice unit $\Delta l_{\rm lb} = 1.25 \times 10^{-4}$m, giving a system with dimensions 4×1.2 cm^2. A fixed fluid injection rate is applied to the left face of the domain with periodic boundary conditions at the top and bottom of the 2D domain. At the right face a constant pressure is applied.

4.2. **Tracer Example.** First, a tracer is considered with the initial concentration in the bulk and matrix fluids set to 0.1 mol/L. Three different orientations of the matrix block are considered with the channel opening pointing to the left, right, and upwards. Because of periodic boundary conditions the case with the channel pointing downwards is equivalent to the case with the channel pointing upwards. The dual continuum model is fit to the flux averaged LB effluent. The effective diffusivity for the matrix was varied to give the best fit to the case with the channel pointing to the left. The resulting fit is shown in Figure 3 (left). The fit is excellent for early and asymptotic times, but deviates at intermediate times. The dual continuum model is unable to capture the the differences in the LB simulations due to the change in orientation of the matrix. Both the single bulk and equivalent continuum models [$\varphi_{\rm ecm} = \epsilon_b \varphi_b + (1-\epsilon_b)\varphi_m = 0.69$] yield breakthrough times that are much too early.

4.3. **Reaction with Linear Kinetics.** Next, reaction is considered for a single component system with linear kinetics. Two rate constants are considered with values of 10^{-7} and 10^{-10} mol cm^{-2} s^{-1}. In this case the value for the effective matrix diffusion constant is taken from the tracer fit and no additional fit parameters are introduced. The reactive surface areas are calculated from the geometry of the system for the bulk and matrix domains as listed in Table 1. The results are shown in Figure 3 (right). For both fast and slow rate constants a stationary state is reached over the path length of the column. However, in the case of the slower rate, equilibrium is not achieved within the column. Clearly, the predictive match

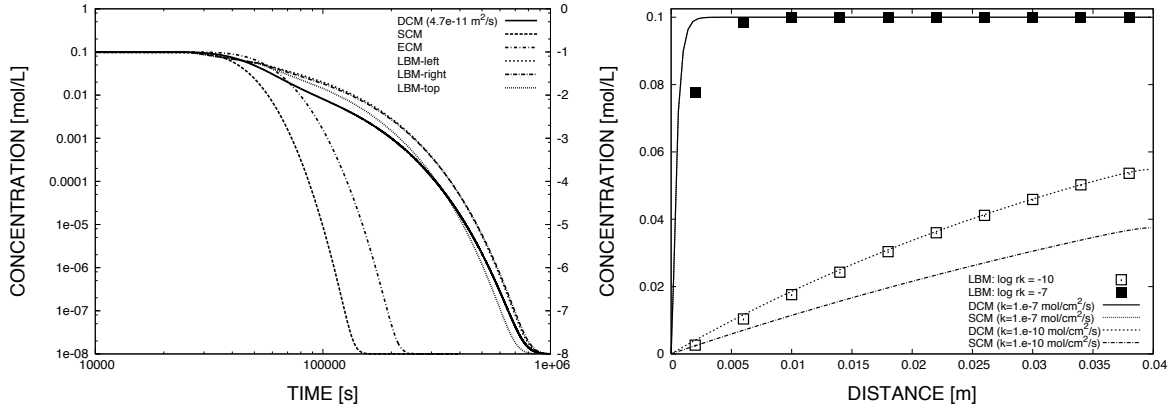

FIGURE 3. Single, equivalent and dual continuum model fits to the tracer LB breakthrough curve (left), to the LB volume averaged spatial concentration profile for linear reaction kinetics (right).

using the dual continuum model for the slower rate constant is excellent. The single continuum model does not enable prediction of the solute concentration without the introduction of effective parameters that differ from the geometric parameters that define the system. A significant contribution from interaction with the matrix enables the dual continuum model to predict the flux-averaged LB result. At the faster rate, the continuum model comes to equilibrium within a shorter distance (shorter equilibration length) compared to the LB result. This is caused by local concentration gradients in the LB simulation that are not captured in the 1D continuum model simulation.

TABLE 1. System parameters for the LB and continuum models.

Property	Units	Bulk	Matrix
System Length (L_b)	cm	4	—
System Width (L_w)	cm	1.2	—
Matrix Block Size (l_m)	mm	—	3.5
Channel Width	mm	—	0.5
Channel Length	mm	—	9.0
Volume Fraction (ϵ_b)	—	0.51	—
Porosity ($\varphi_b,\ \varphi_k$)	—	1	0.367
Diffusivity ($D_b,\ D_k$)	$\mathrm{m^2\ s^{-1}}$	10^{-9}	4.7×10^{-11}
Surface Area ($A_b,\ A_k$)	$\mathrm{cm^{-1}}$	5.625	15.102
Darcy Velocity ($q_b,\ q_k$)	$\mathrm{m\ y^{-1}}$	14.4	0

4.4. **Fractured Medium.** Figure 4 shows averaged concentration at $t = 1.3 \times 10^4$s, for $k = 10^{-10}$ mol/cm^2/s, and log$K$=1, along flow direction for both the LB simulation and discrete fracture model (DFM), with and without dispersion. The averaging is taken over vertical slabs. For macroscopic parameters needed in the DFM simulations, the surface area and matrix porosity are obtained directly from the geometry. The permeability of and dispersivity in the fracture are calculated using cubic law and Taylor dispersion for non-reactive solute, respectively. The permeability of the matrix is calcuated in a separate LB simualtion of flow through the matrix only (without fracture). The tortuosity of the matrix, however, is determined by comparing a pore scale LB simulation with continuum scale simulations with different tortuosity values of pure diffusion through the matrix. Clearly, the DFM simulation with dispersion matches that of the LB simulation very well.

5. CONCLUSION

In order to capture the effects of pore-scale processes caused by dead-end pores or secondary porosity, a dual or multiple continuum formation is required. However, even a multiple continuum model may not be able to capture the effects of pore scale concentration gradients resulting from fast reaction rates. Upscaling pore scale simulations using the LB method to the continuum scale suggests that for sufficiently slow rates of reaction such that concentration gradients do not occur with a single pore, volume averaging is adequate to obtain approximate specific mineral surface areas at different scales. However, the LB simulations also indicate that a single continuum representation generally will not suffice, but that a dual or multiple continuum formulation is needed. This is because of the presence of different grain sizes and compositions, dead-end pores and secondary porosity. By fitting a pore-scale tracer breakthrough curve, it was possible to predict the system behavior in the presence of reaction. In fractured media a dual continuum approach is certainly required for scales that include many fractures within a control volume, whereas for finer scales that explicitly resolve individual fractures a discrete fracture model may suffice.

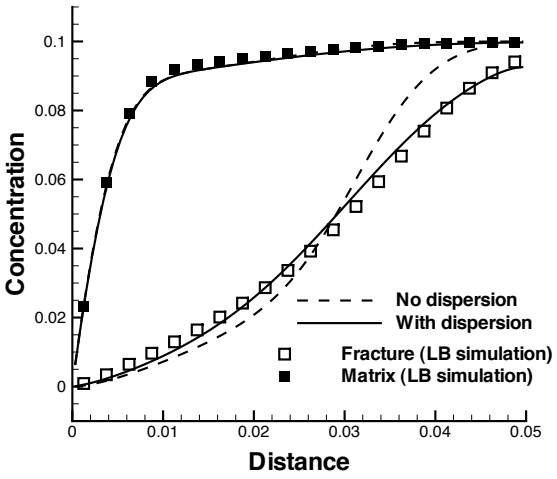

FIGURE 4. Spatial distribution of averaged LB and DFM concentration.

REFERENCES

Chen and Doolen, 1998. Chen, S., and G.D. Doolen (1998), Lattice Boltzmann method for fluid flows, *Annu. Rev. Fluid Mech., 30,* 329–364.

Kang et al., 2004. Kang, Q., D. Zhang, P. C. Lichtner, and I. N. Tsimpanogiannis (2004), Lattice Boltzmann model for crystal growth from supersaturated solution, *Geophys. Rev. Lett., 31,* L21604.

Kang et al., 2005. Kang, Q., I. N. Tsimpanogiannis, D. Zhang, and P. C. Lichtner (2005), Numerical modeling of pore-scale phenomena during CO2 sequestration in oceanic sediments, *Fuel Proce. Tech., 86,* 1647.

Kang et al., 2006. Kang, Q., P. C. Lichtner and D. Zhang (2006), Lattice Boltzmann pore-scale model for multicomponent reactive transport in porous media, *J. Geophys. Res.*, in press.

Lichtner, 1985. Lichtner, P. C. (1985), Continuum model for simultaneous chemical reactions and mass transport in hydrothemal systems, *Geochimica et Cosmochimica ACTA, 49,* 779–800.

Lichtner, 1996. Lichtner, P. C. (1996), Continuum formulation of multicomponent-multiphase reactive transport, *Reviews in Mineralogy, 34, Reactive Transport in Porous Media,* 1–81.

Lichtner, 2000. Lichtner, P.C. (2000) Critique of Dual Continuum Formulations of Multicomponent Reactive Transport in Fractured Porous Media, Dynamics of Fluids in Fractured Rock. Geophys. Monograph, 122, 281–298.